Foetal Age and Weight Determination Using a Lateral Interaction Inspired Net

A. Fernández-Caballero[1], J. Mira[2], F.J. Gómez[1], and M.A. Fernández[1]

[1] Departamento de Informática, Universidad de Castilla-La Mancha, 02071- Albacete, Spain
{caballer, fgomez, miki}@info-ab.uclm.es
[2] Departamento de Inteligencia Artificial, UNED, c/ Senda del Rey 9, 28040- Madrid, Spain
jmira@dia.uned.es

Abstract. The clinical estimate of the foetal weight is probably one of the most difficult parameters to obtain in the prenatal control. Only very accurate foetal body measurements reflect the gestation age and the weight of the foetus. A model is presented that performs an automated foetal age and weight determination from ultrasound by means of biparietal diameter, femur lenght and abdominal circumference parameters. The model proposed in this paper exploits the data in the images in three general steps. The first step is image pre-processing, to highlight useful data in the image and suppress noise and unwanted data. The next step is image processing, which results in forming regions that can correspond to structures or structure parts. The last step is image understanding, where knowledge on the specific problem is injected.

1 Introduction

By means of the prenatal control it is possible to watch over the evolution of the pregnancy. The general objectives of the prenatal control are: (a) to identify factors of risk, (b) to diagnose the gestation age, (c) to diagnose the foetal state, and, (d) to diagnose the maternal state.

The elements that are used for the calculation of the gestation age are the amenorrhoea time, starting from the first day of the last menstruation, and the uterine size. The ignorance of the gestation age constitutes for itself a factor of risk. That's why it is so important to have ultrasound resources.

The clinical elements that allow to evaluate the foetal state are: (a) the foetal heartbeats, (b) the foetal movements, (c) the uterine size, (d) the clinical estimate of the foetal weight, and, (e) the clinical estimate of the amniotic liquid volume. The heartbeats can be identified with ultrasound from the tenth week of pregnancy. The uterine size may be obtained using a flexible ribbon and permits to estimate the foetal size in each prenatal control. The clinical estimate of the foetal weight is probably one of the most difficult parameters to obtain in the prenatal control, since it demands a good piece of experience for its determination. The error of estimate of the foetal weight in pregnancy during the third trimester is about a ten percent.

The need for a quick and easy method for estimating foetal weight in uterus has been clearly established by a great number of professionals. Estimates by abdominal palpation and foetal hormone production have proved to be of limited value [17]. Only very accurate measurements of the foetus allow dating of the pregnancy and serial assessment of foetal growth in comparison with previous measurements.

2 Foetus age and weight determination

2.1 The most important measures

In the 1980s the assessment of intrauterine growth retardation using ultrasonic parameters was the subject of many research papers. The aim to predict foetal weight from computer-generated equations produced normalised tables for every measurable parts of the foetal body [15] [18]. The arrival of the real time scanners have added further impetus to ultrasound techniques and have established ultrasound as the most important imaging modality on Obstetrics and Gynaecology.

The advent of ultrasound in Obstetrics has created the new speciality called prenatal diagnosis that has developed since its early conception. Foetal body measurements reflect the gestation age of the foetus. The following measurements are usually made:

1. The crown-rump length (CRL). This measurement can be made between 7 to 13 weeks and gives very accurate estimation of the gestation age.
2. The biparietal diameter (BPD) and the head circumference (HC). The biparietal diameter is the diameter between the two sides of the head. This is measured after 13 weeks. The HC is less often used than the BPD.
3. The femur length (FL). This is the measure of the longest bone in the body and reflects the longitudinal growth of the foetus. Its usefulness is similar to the BPD.
4. The abdominal circumference (AC). This is the single most important measurement to make in late pregnancy. It reflects more of foetal size and weight than age. Serial measurements are useful in monitoring growth of the foetus.

2.2 The domain knowledge

Expert or knowledge-based systems are the commonest type of Artificial Intelligence in Medicine system in routine clinical use. They contain medical knowledge, usually about a very specifically defined task [4]. This is precisely our aim in this paper. So we are going to explain the domain knowledge on the measures described before. But we have restricted to those measures characteristic of the second and third pregnancy trimester.

The BPD remains the standard against which other parameters of gestation age assessments are compared. The BPD should be measured as early as possible after 13 weeks of dating. The problem of head moulding as it relates to the accuracy BPD of the foetal head has long been recognised. The anatomical landmarks used to ensure the accuracy and reproducibility of the measurement include: (a) a midline falx, (b) the thalami symmetrically positioned on either side of the falx, (c) visualisation of the septum pellucidum on one third the front-occipital distance. The BPD increases from about 2.4 cm at 13 weeks to about 9.5 cm at term. A wrong measurement plane can produce errors up to 2 cm.

The FL is a mandatory measurement. By convention, measurement of the FL is considered accurate only when the image shows two blunted ends. The lateral surface of the femur is always straight and the medial surface is always curved. The use of FL in dating is similar to the BPD, and is not superior unless a good plane cannot be obtained. The FL increases from about 1.5 cm at 14 weeks to about 7.8 cm at term.

Measurement of the AC should be made as accurately as possible. The best plane is the one in which the portal vein is visualised in a tangential section. The plane in which the stomach is visualised is also acceptable. The outer edge of the circumference is measured. With a good AC, one will be able to arrive at a very accurate foetal weight. Indeed, the weight of the foetus at any gestation age can be estimated with great accuracy using polynomial equations containing the BPD, FL and AC. One such possible equation is [15]:

$$\log_{10} W = -1.7492 + 0.166 \cdot BPD + 0.046 \cdot AC - 0.002646 \cdot AC \cdot BPD \qquad (\mathbf{1})$$

3 The model

The model proposed in this paper falls into the data-driven approaches and exploits the data in the images in three general steps. The first step is image pre-processing, to highlight useful data in the image and suppress noise and unwanted data. To fulfil this step some standard image filters have been employed. The next step is image processing, which results in forming regions that can correspond to structures or structure parts. Here, we have used the Lateral Interaction in Accumulative Computation Model [5]. This model formally splits into four stages, as depicted on figure 1. The last step is image understanding, where all knowledge on the specific problem is injected.

Precise segmentation of underlying structures in medical images is a top cue. The existing work on image segmentation can be typically categorised into two basic approaches [2]: region-based methods relying on the homogeneity of spatially and temporally features, and, gradient-based methods looking for some kinds of boundaries. Our approach integrates both concepts to limit the intrinsic problems of both methods.

Step 1. Image pre-processing by standard filters

A major problem in medical image analysis is the potential variability in the image characteristics and object appearance. This first step aims to maximally improve the input images (ultrasonography images) in order to optimise the image processing step in time and quality. This problem has firstly been addressed by selecting a set of well-known standard filters used in image pre-processing.

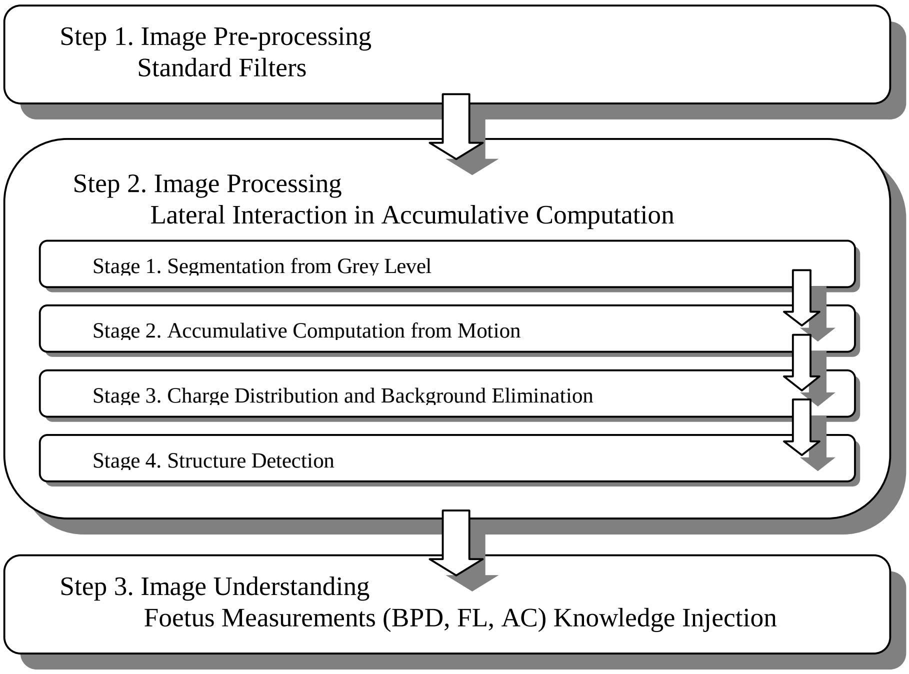

Figure 1. The model

The final goal of step 1 is to reduce the textured aspect of the embryonic ultrasonography images and to concentrate on the desired regions or structures. In our particular cases, we have to highlight any aspects of the structure of the skull, the femur and the abdomen, whereas the rest of the image has to be considered as undesired background.

Step 2. Image processing by lateral interaction in accumulative computation

By image processing in automatic analysis of medical images we include all those techniques that help in diagnostic. We could mention among others: (a) objective quantitative parameter extraction on shape and texture, (b) change detection among two images, (c) information fusion from several modalities, (d) comparison of images from two different patients, (e) probabilistic anatomical and functional atlas construction, (f) motion measures of dynamic organs, and, (g) dynamic visualisation of images [1].

Our model at this step 2 takes advantage of all information concerning motion analysis in foetal ultrasound. Motion analysis in dynamic image sequences is a really hard matter [9] and some approaches have been used in medicine [3] [10] [14] [8] [16]. This generic model is based on a neural architecture, with recurrent and parallel computation at each specialised layer, and sequential computation between consecutive layers. The model is based on an accumulative computation function [6] [7], followed by a set of co-operating lateral interaction processes performed on a functional receptive field organised as centre-periphery over linear expansions of their input spaces [11] [12] [13]. The model also incorporates the notion of double time scale at accumulative computation level present at sub-cellular micro-computation [7].

Any stage of step 2 is implemented as a neural layer as depicted on figure 2. This figure shows the intra- and interconnections of any element *(i,j)* of any one of the four layers. At each layer *n*, element *(i,j)* receives an input from element *(i,j)* of layer *n-1* and sends an output to element *(i,j)* of layer *n+1* at global time scale *t*. At local time scale *T* $(t = k \cdot T)$, intraconnectios take place in the sense that data present at element *(i,j)* is exchanged with its neigbours data. These neighbours are *(i-1,j), (i+1,j), (i,j-1)* and *(i,j+1)*.

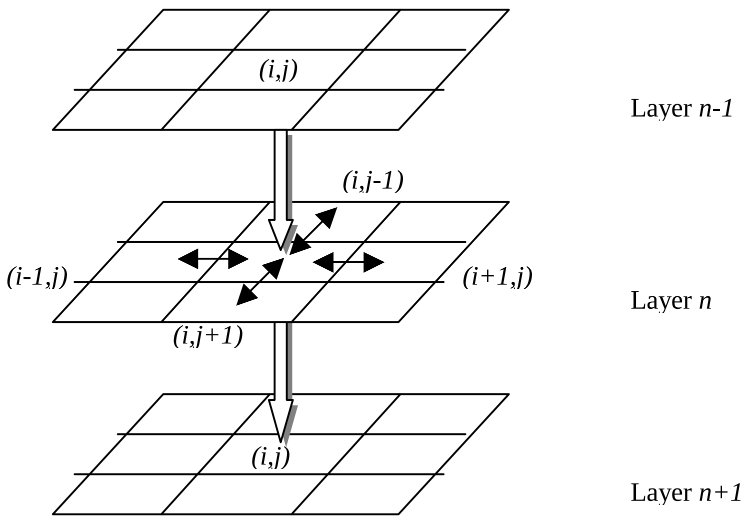

Figure 2. A module's connections

Stage 2.1. Segmentation from grey level

The aim of this stage 2.1,corresponding to layer 1, is to determine in what grey level stripe *GLS* a given pixel *(i,j)* falls. We consider the pre-processed image to segment to be the input to this stage.

$$GLS_k(i,j,t) = \begin{cases} 1, & if\ GL(i,j,t) \in [(256/n)k, (256/n)(k+1)[\\ 0, & otherwise \end{cases}$$

where n = number of grey level stripes

k = grey level stripes

GL = grey level

Stage 2.2. Accumulative computation from motion

Supstep 2.2 (layer 2) makes use of *n* sub-layers, one for each of the chosen grey level stripes. This stage incorporates the described lateral interaction mechanisms. We are to explain how this stage works on each of the central elements *(i,j)* at any sub-layer *k*. This stage is capable of modelling the motion on the image, starting from the pixel's grey level stripe and the element's state or permanence value *PM*. At each time instant *t*, the permanence value is obtained in two steps. (1) At global time, a complete discharge (v_{dis}), a saturation (v_{sat}) or partial discharge (v_{dm}) due to the motion detection, that's to say, due to a change in the grey level stripe, and, (2) at local time, a partial re-charge (v_{rv}) due to the lateral interaction on the partially charged elements that are directly or indirectly connected to maximally charged elements.

$$PM_k(i,j,t) = \begin{cases} v_{dis}, & if\ GLS_k(i,j,t) \equiv 0 \\ v_{sat}, & if\ GLS_k(i,j,t) \equiv 1 \cap GLS_k(i,j,t-\Delta t) \equiv 0 \\ PM_k(i,j,t-\Delta t) - v_{dm}, & if\ GLS_k(i,j,t) \equiv 1 \cap GLS_k(i,j,t-\Delta t) \equiv 1 \end{cases}$$

$$PM_k(i,j,T) = PM_k(i,j,T-\Delta T) + v_{rv}$$

Stage 2.3. Charge distribution and background elimination

Starting from the values of the permanence memory *PM* in each pixel, it is possible to obtain the silhouette of all the parts of a moving object starting from the spots left by the different grey level stripes. That’s why, at this point, the charge of the permanence values is homogeneously distributed among all the elements that have the same grey level value, provided that they are directly or indirectly connected to each other through the necessary lateral interaction mechanisms of recurrent type. This way, a double objective will be obtained at this layer 3. First, the one of diluting the charge due to the background false motion detected on the image, only keeping the movement of the desired structures of the scene. And secondly, the one of obtaining a common parameter to all the elements of a same part of a structure.

$$C_k(i,j,t) = PM_k(i,j,t)$$

$$\begin{aligned} C_k(i,j,T) = {}^1\!/_5\,(&C_k(i,j,T-\Delta T) + C_k(i-1,j,T-\Delta T) + C_k(i+1,j,T-\Delta T) + \\ &+ C_k(i,j-1,T-\Delta T) + C_k(i,j+1,T-\Delta T)) \end{aligned}$$

Stage 2.4. Structure detection

So far, by means of the necessary co-operative calculation mechanisms, attention has been captured on anything that has moved at any grey level stripe, and motion due to the background has been eliminated. Now, at this layer 4, it is necessary to fix as a new objective to distinguish the different objects that conform the different parts of the structures obtained on a grey level stripe basis (spots). The discrimination of these structures is also performed by lateral interaction of recurrent type. Now, we will no longer work with sub-layers, but rather all the information of the *n* sub-layers of stage

2.3 is integrated in a single layer. In this stage 2.4, the charge again will be homogeneously distributed among all the elements that have a charge value superior to a minimum threshold and that are physically connected to each other.

$$S(i, j, t) = \max(C_k(i, j, t))$$

$$S(i, j, T) = \tfrac{1}{5}\,(S(i, j, T-\Delta T) + S(i-1, j, T-\Delta T) + S(i+1, j, T-\Delta T) + \\ + S(i, j-1, T-\Delta T) + S(i, j+1, T-\Delta T))$$

Step 3. Image understanding by foetus measurements knowledge injection

In this last step all general knowledge on foetus measurements to obtain the age and the weight of the embryo is injected. Four stages are needed to obtain both parameters. (1) BPD determination, (2) FL determination, (3) AC determination, and, (4) age and weight calculation. We next offer the rules as applied from domain knowledge.

```
BPD determination

Locate Skull;
Locate Biparietal extremities;
Obtain BPD;

FL determination

Locate Femur;
Locate Femur extremities;
Obtain FL;

AC determination

Locate Abdomen;
Locate Abdomen circumference;
Obtain AC;

Age and weight calculation

Find Age-BPD from BPD-Chart; Output Age-BPD;
Find Age-FL from FL-Chart;   Output Age-FL;
Calculate Weight from Equation 1;
```

4 Learning in lateral interaction in accumulative computation

Learning in lateral interaction in accumulative computation starts from the knowledge of the influence of the basic parameters of the model. Learning in lateral interaction in accumulative computation model consists in adjusting the parameters of the diverse layers to offer the best processing result of the image sequence when obtaining the silhouettes of moving elements present in the scene.

During the learning process, previous to the normal operation process, the architecture is offered an input image sequence, as well as the following reinforcement parameters (see figure 3):

- *Number of moving elements (S_m)* to be detected in the sequence
- *Maximum size of a silhouette (S_{max})* to be detected in the sequence
- *Minimum size of a silhouette (S_{min})* to be detected in the sequence

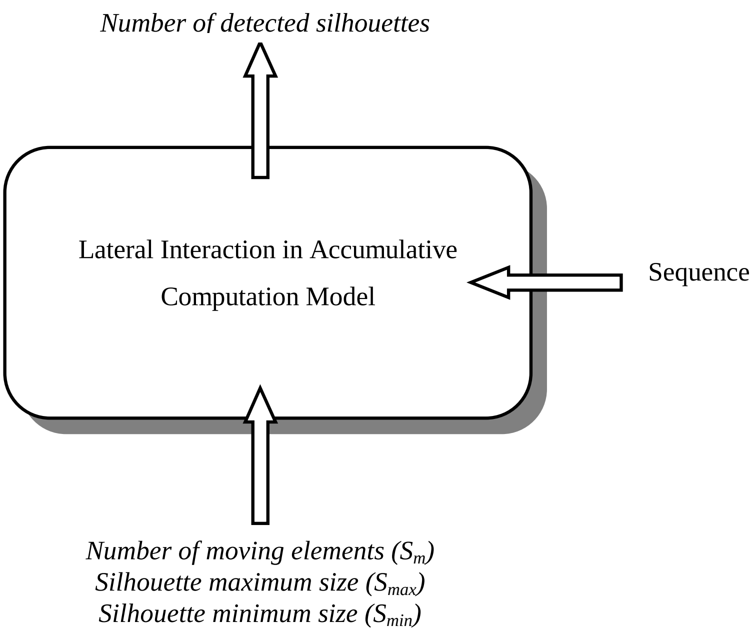

Figure 3. Inputs and outputs during learning phase

Due to its simplicity, it doesn't seem necessary to explain the reinforcement parameter *Number of moving elements (S_m)*. The other two parameters arise from the domain knowledge of lateral interaction in accumulative computation model. It is indispensable to introduce parameters *Maximum size of a silhouette (S_{max})* and *Minimum size of a silhouette (S_{min})* to capture the attention on those objects whose silhouette falls between these two magnitudes.

Learning turns, in our case, into an iterative process where, for a given scene, the model is nurtured by a same image sequence, just modifying the basic parameters until the number of silhouettes obtained at layer 4 is close enough to *Number of moving elements (S_m)*. The output obtained at layer 4 is *called Number of Detected Silhouettes (S_d)*.

The basic parameters of lateral interaction in accumulative computation model have been classified into two groups:

- *Parameters with constant values that don't evolve during the learning phase.* These are v_{dis} (minimum permanency value) and v_{sat} (maximum permanency value) at layer 2.
- *Parameters with values that do evolve during the learning phase.* These are: n (number of gray level bands) at layer 1; v_{dm} (discharge value due to motion detection), v_{rv} (recharge value due to vicinity), and, θ_{per} (threshold) at layer 2; θ_{ch} (threshold) at layer 3; θ_{obj} (threshold) at layer 4.

So, we use an error minimization function in the sense that the problem is now to find a procedure of estimating a set of values that best leads to the desired solution. In other words, we have to look for a set of optimal values

$$C^* = \left(n^*, \, v^*{}_{dm}, \, v^*{}_{rv}, \, \theta^*{}_{per}, \, \theta^*{}_{ch}, \, \theta^*{}_{obj}\right)$$

that minimize error function

$$E = \left| \, S_m - \frac{1}{k} \sum_{t=0}^{k} S_d(t) \, \right|$$

where k is the number of images that form the learning sequence,

S_m is the number of moving elements to be detected (constant through the whole training sequence),

S_d *(t)* is the number of detected silhouettes at time instant t.

5 Results

The model has been tested with a series of ultrasound images of Sara Gómez at a gestation age of aproximately 18 weeks. This important information has helped us to confirm the results of our model. You may appreciate the results of the image pre-processing and image processing steps of some of Sara’s skull, femur and abdomen images on figures 4, 5 and 6, respectively.

You may appreciate on columns (a)the original input images. Column (b) presents the pre-processed images where only a few pixels of interest are taken. Lastly, on column (c) you may observe how our proposed model is capable of obtaining more significant information from the described region growing technique. Finally, table 1 shows the results of the image understanding step.

These results suggest that the proposed model is able to obtain accurate data for an automated foetal age and weight determination.

(a) (b) (c)

Figure 4. Application of image processing model to Sara's skull. (a) Original image. (b) Result of pre-processing step. (c) Result of processing step.

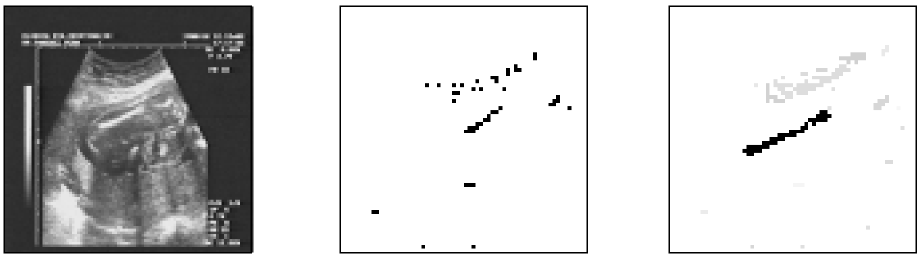

(a) (b) (c)

Figure 5. Application of image processing model to Sara's femur. (a) Original image. (b) Result of pre-processing step. (c) Result of processing step.

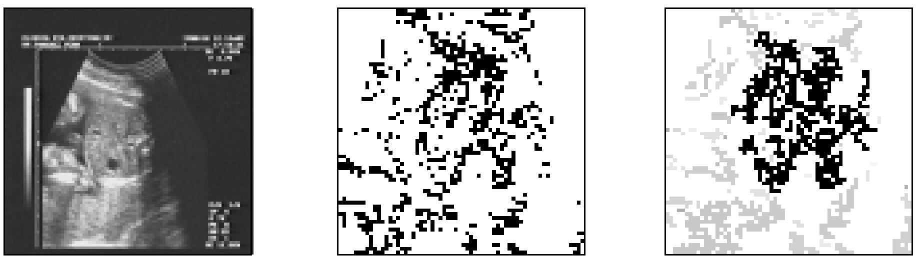

(a) (b) (c)

Figure 6. Application of image processing model to Sara's abdomen. (a) Original image. (b) Result of pre-processing step. (c) Result of processing step.

Table 1. Results of image understanding model to Sara's ultrasound images

Computed Age-BPD	= 17.6	weeks
Computed Age-FL	= 18.2	weeks
Calculated Weight	= 0.231	kg

References

1. Ayache, N.: L'analyse automatique des images médicales. Etat de l'art et perspectives. Technical Report 3364, INRIA, France (1998)
2. Ballard, D.H., Brown, C.M.: Computer Vision. Prentice Hall (1982)
3. Benayoun, S., Ayache, N.: 3D motion analysis using differential geometry constraints. International Journal of Computer Vision 26:1 (1998) 25-40
4. Coiera, E.: Guide to Medical Informatics, the Internet and Telemedicine. Chapman & Hall Medical (1997)
5. Fernández-Caballero, A.: Modelos de interacción lateral en computación acumulativa para la obtención de siluetas. Unpublished Ph.D. dissertation (2001)
6. Fernández, M.A., Mira, J.: Permanence memory: A system for real time motion analysis in image sequences. IAPR Workshop on Machine Vision Applications, MVA'92 (1992) 249-252
7. Fernández, M.A., Mira, J., López, M.T., Alvarez, J.R., Manjarrés, A., Barro, S.: Local accumulation of persistent activity at synaptic level: Application to motion analysis. In: Mira, J., Sandoval, F. (eds.): From Natural to Artificial Neural Computation, IWANN'95, LNCS 930. Springer-Verlag (1995) 137-143
8. Kraitchman, D., Young, A., Chang, C.N., Axel, L: Semi-automatic tracking of myocardial motion in MR tagged images. IEEE Transactions on Medical Imaging 14:3 (1995) 422-433
9. McInerney, T., Terzopoulos, D.: Deformable models in medical image analysis: A survey. Medical Image Analysis 1:2 (1996) 91-108
10. McVeigh, E.R.: MRI of myocardial function: Motion tracking techniques. Magnetic Resonance Imaging 14:2 (1996) 137-150
11. Mira, J., Delgado, A.E., Alvarez, J.R., de Madrid, A.P., Santos, M.: Towards more realistic self contained models of neurons: High-order, recurrence and local learning. In: Mira, J., Cabestany, J., Prieto, A. (eds.): New Trends in Neural Computation, IWANN'93, LNCS 686. Springer-Verlag (1993) 55-62
12. Mira, J., Delgado, A.E., Manjarrés, A., Ros, S., Alvarez, J.R.: Cooperative processes at the symbolic level in cerebral dynamics: Reliability and fault tolerance. In: Moreno-Díaz, R., Mira, J. (eds.): Brain Processes, Theories and Models. The MIT Press (1996) 244-255
13. Moreno-Díaz, R., Rubio, F., Mira, J.: Aplicación de las transformaciones integrales al proceso de datos en la retina. Revista de Automática 5 (1969) 7-17
14. Rueckert, D., Sánchez-Ortiz, G.I., Burger, P.: Motion and deformation analysis of the myocardium using density and velocity encoded MR images. In: Proceedings of the 10th International Symposium and Exhibition on Computer Assisted Radiology (1996)
15. Shephard, M.J., Richards, V.A., Berkowitz, R.L., Hobbins, J.C.: An evaluation of two equations for predicting fetal weight by ultrasound. American Journal of Obstetrics and Gynecology (1982) 142:147.
16. Shi, P., Robinson, G., Chakraborty, A., Staib, L. Constable, R., Simusas A., Duncan, J.: A unified framework to assess myocardial function from 4D images. In: Computer Vision, Virtual Reality and Robotics in Medicine, LNCS 905. Springer-Verlag (1995) 327-337
17. Warsof, S.L., Gohari, P., Berkowitz, R.L., Hobbins, J.C.: The estimation of fetal weight by computer-assisted analysis. American Journal of Obtetrics and Gynecology 128:8 (1977) 881-892
18. Woo, J.S.K.: Obstetric ultrasound: A comprehensive guide to ultrasound scans in pregnancy. http://www.ultrasound.net/ (2000)